Published in final edited form as:
Biochemistry. 2012 June 5; 51(22): 4453–4462. doi:10.1021/bi3003204.

Characterization of the [2Fe-2S] cluster of the *Escherichia coli* transcription factor IscR†

Angela S. Fleischhacker[#], **Audria Stubna**[§], **Kuang-Lung Hsueh**[‡], **Yisong Guo**[§], **Sarah J. Teter**[#], **Justin C. Rose**[#], **Thomas C. Brunold**[⊥], **John L. Markley**[‡], **Eckard Münck**[§], and **Patricia J. Kiley**[#,*]

[#]Department of Biomolecular Chemistry, University of Wisconsin, Madison, Wisconsin, 53706

[‡]Department of Biochemistry, University of Wisconsin, Madison, Wisconsin, 53706

[§]Department of Chemistry, Carnegie Mellon University, Pittsburgh, Pennsylvania, 15213

[⊥]Department of Chemistry, University of Wisconsin, Madison, Wisconsin, 53706

Abstract

IscR is a Fe-S cluster-containing transcription factor involved in a homeostatic mechanism that controls Fe-S cluster biogenesis in *Escherichia coli*. Although IscR has been proposed to act as a sensor of the cellular demands for Fe-S cluster biogenesis, the mechanism by which IscR performs this function is not known. In this study, we investigated the biochemical properties of the Fe-S cluster of IscR to gain insight into the proposed sensing activity. Mössbauer studies revealed that IscR contains predominantly a reduced $[2Fe\text{-}2S]^{1+}$ cluster *in vivo*. However, upon anaerobic isolation of IscR some clusters became oxidized to the $[2Fe\text{-}2S]^{2+}$ form. Cluster oxidation did not, however, alter the affinity of IscR for its binding site within the *iscR* promoter *in vitro*, indicating that cluster oxidation state is not important for regulation of DNA binding. Furthermore, characterization of anaerobically isolated IscR using resonance Raman, Mössbauer, and NMR spectroscopies leads to the proposal that the [2Fe-2S] cluster does not have full cysteinyl ligation. Mutagenesis studies indicate that, in addition to the three previously identified cysteine residues (Cys92, Cys98, and Cys104), the highly conserved residue His107 is essential for cluster ligation. Thus, these data suggest that IscR binds the cluster with an atypical ligation scheme of three cysteines and one histidine, a feature that may be relevant to the proposed function of IscR as a sensor of cellular Fe-S cluster status.

The *Escherichia coli* transcription factor IscR regulates the expression of over 40 genes, including the *isc* operon encoding IscR itself and the Isc proteins responsible for Fe-S cluster biogenesis (1). IscR, which was found to contain a [2Fe-2S] cluster upon anaerobic isolation, requires a functional Isc pathway to repress *isc* operon transcription (2), suggesting an intimate link between the Fe-S cluster occupancy of IscR and its function as a repressor of the Isc pathway. The noted connection further led to the hypothesis that IscR acts as a sensor of the cellular demands for Fe-S cluster biogenesis (2, 3). Although the mechanism of sensing is unknown, atypical Fe-S cluster protein properties such as inefficient Fe-S cluster acquisition by IscR or unusual sensitivity to oxidants could make the Fe-S cluster occupancy of IscR sensitive to the general cellular demands for Fe-S cluster biogenesis. Characterization of the biochemical properties of the Fe-S cluster of IscR is an

†This work was supported by the National Institutes of Health grants F32GM085987 (A. S. F.), GM45844 (P. J. K.), R01GM58667 (J. L. M.), P41RR02301 (J. L. M.), and EB001474 (E. M.).

*To whom correspondence should be addressed: Patricia J. Kiley 4204C Biochemical Sciences Building 440 Henry Mall Madison, Wisconsin 53706 pjkiley@wisc.edu Tel 608-262-6632 Fax 608-262-5253.

important first step toward the development of a detailed understanding of the sensing mechanism employed by IscR.

One fundamental question regarding the cluster-bound state of IscR involves the amino acid side chains required for cluster ligation. Most [2Fe-2S] clusters have all cysteinyl $(Cys)_4$ ligation. Notable exceptions are the Rieske proteins, which have [2Fe-2S] clusters featuring $(Cys)_2(His)_2$ ligation. Cys92, Cys98, and Cys104 are the only cysteines in IscR, and all three have been shown by mutagenesis studies to be necessary for the formation of holo-protein (4, 5). Furthermore, both [2Fe-2S] and clusterless IscR were found to exist as homodimers in solution (5). Therefore, if the cluster of IscR had full cysteinyl ligation typical of Fe-S clusters, the cluster would have to bridge the subunits of the dimer. Consistent with this model, anaerobically isolated IscR was ~50% occupied with cluster (5). However, the EPR *g* values for *E. coli* $[2Fe\text{-}2S]^{1+}$-IscR of 1.99, 1.93, and 1.88 (2) are inconsistent with all cysteinyl ligation of the Fe-S cluster. The *g* values of $[2Fe\text{-}2S]^{1+}$ clusters are influenced by ligand coordination (6, 7). Importantly, the average *g* value (g_{av}) ~1.93 for $[2Fe\text{-}2S]^{1+}$-IscR is lower than values reported for proteins that ligate [2Fe-2S] clusters via four cysteines (g_{av} ~ 1.97), suggesting that the IscR-bound cluster has an unusual ligation scheme.

IscR is a member of the Rrf2 family of transcription factors, predicted to contain a characteristic winged helix-turn-helix DNA-binding domain (PF02082, (8)). The family members are not well characterized, but the presence of conserved cysteines in several of them suggests that a subset of these proteins may ligate Fe-S clusters. While previous studies have shown that IscR from *E. coli* contains a [2Fe-2S] cluster that can be reversibly oxidized and reduced (2), neither the type of cluster that is present *in vivo*, nor its *in vivo* oxidation state have been examined. Such information is of increasing importance as differences in isolation methods have emerged as a factor affecting the type of isolated cluster because of the potential for cluster conversions. For example, recent studies of a related transcription factor in the Rrf2 family, the NO sensor NsrR, raised the question of whether the functional form of NsrR contains a [2Fe-2S] or a [4Fe-4S] cluster (9).

In this study, cluster-bound IscR of *E. coli* was characterized *in vivo* and *in vitro* to further our understanding of the function of IscR as a sensor of the Fe-S cluster status of the cell. First, to determine the nature of the cluster bound to IscR *in vivo*, Mössbauer spectra were collected of IscR in whole cells. A combination of resonance Raman, NMR, and Mössbauer spectroscopies were then used to characterize the Fe-S cluster of isolated IscR and to identify its ligands. In conjunction, mutagenesis studies were performed to explore possible ligation schemes. The effects of substituting IscR residues with alanine or other amino acids were analyzed *in vitro* by quantifying Fe-S cluster occupancy of the anaerobically isolated IscR variants and *in vivo* by monitoring the ability of the IscR variants to repress the *iscR* promoter in a *lacZ* reporter strain. Finally, we examined the effect of the Fe-S cluster oxidation state on DNA binding by IscR using fluorescence polarization assays. The results presented lead to the proposal that *E. coli* IscR has an unusual $(Cys)_3(His)_1$ Fe-S cluster ligation scheme, which may be relevant to the ability of IscR to function as a sensor of the cellular Fe-S cluster status. A similar ligation scheme has recently been proposed for the Fra2-Grx3 heterodimeric complex, which is involved in iron regulation in yeast and has possible sensor functions (10, 11).

Methods

Mössbauer spectroscopic analysis of anaerobically isolated IscR

Wild type IscR was isolated anaerobically from *E. coli* strain PK7901 (BL21Δ*crp-bs990*Δ*fnr* harboring pPK6161) as described previously (1) except that cells were grown in Chelex-treated glucose M9 media supplemented with 10 μM ^{57}Fe-ferrous

ethylenediammonium sulfate, and a Poly-CatA ion exchange column chromatography step was used in place of heparin ion-exchange. An HPLC Poly-CatA ion exchange column was equipped with a column chiller and attached to a Beckman HPLC system in an anaerobic chamber (12). The sample was loaded and subsequently washed with 95 mL 50 mM Tris buffer, pH 7.4, containing 0.1 M KCl, 10% glycerol, and 1 mM dithiothreitol. The protein was eluted with a 12 mL gradient (2% to 50%) of 50 mM Tris buffer, pH 7.4, containing 1.0 M KCl, 10% glycerol, and 1 mM dithiothreitol at 0.5 mL min^{-1}. The eluted protein was subsequently purified and concentrated over size exclusion and BioRex-70 columns, respectively, as described previously (1), except that 50 mM Tris buffer, pH 7.4, was used in place of HEPES buffer. The protein was subsequently transferred to a Mössbauer sample cup, and spectra were recorded of the as-purified IscR sample. The sample then was thawed and exposed to air for 5 minutes, and spectra were recorded. Finally, the sample was thawed in an anaerobic chamber, and 10 μL of 35 mM dithionite was added. After 30-60 s with stirring, the sample was rapidly frozen and analyzed by Mössbauer spectroscopy, as described previously (13).

Whole cell Mössbauer spectroscopy

Cell cultures were grown, subsequently prepared for, and analyzed by whole cell Mössbauer spectroscopy, as described previously (14, 15) with minor modifications. Strain PK7901 over-expressing IscR or a strain lacking over-expressed IscR (BL21 + pET11a) were grown in the presence of 10 μM ^{57}Fe-ferrous ethylenediammonium sulfate (12), and the cell pellet was washed with 50 mM Tris buffer, pH 7.4, containing 0.1 M KCl and 10% glycerol before the sample was transferred to a Mössbauer sample cup and frozen on dry ice.

Resonance Raman spectroscopy

Wild type IscR was isolated from strain PK7901 as described for Mössbauer spectroscopy. Spectra were recorded upon excitation with an Ar^+ ion laser (Coherent I-305) with incident power in the 50-100 mW range. The scattered light was collected using a ~135° backscattering arrangement, dispersed by a triple monochromator (Acton Research, equipped with 300, 1200, and 2400 grooves/mm gratings) and analyzed with a deep depletion, back-thinned CCD camera (Princeton Instruments Spec X: 100BR). All spectra were collected at 77 K on frozen protein samples contained in NMR tubes that were immersed in an N_2(l)-filled EPR dewar to prevent photo-degradation.

Isolation of IscR for visible spectroscopy, NMR spectroscopy, and binding assays

IscR and IscR variants were isolated under anaerobic conditions using heparin-ion exchange, gel filtration, and BioRex-70 column chromatographies (1). Protein concentration (reported on a per-monomer basis) and iron content were determined colorimetrically (2). Absorption spectra of IscR (isolated from strain PK8581) and IscR variants were recorded anaerobically in 10 mM HEPES buffer, pH 7.2, containing 0.2 M KCl in sealed cuvettes (12).

Strain construction and β-galactosidase assays

Chromosomally-encoded mutants of *iscR* were constructed as described previously (5). Three independent isolates of each strain were grown in MOPS minimal media with 0.2% glucose under anaerobic conditions (1) to an $O.D._{600}$ of ~0.1 and assayed for β-galactosidase activity (16).

Preparation of ^{15}N-labeled protein samples

Wild type (WT) IscR was isolated from strain PK8581 grown with ^{15}N-labeled NH_4Cl (Cambridge Isotope Laboratories) and without the addition of casaminoacids to generate a

uniformly ^{15}N-labeled IscR sample: [U-^{15}N]-IscR(WT). A second sample was prepared from cells grown by the same protocol, except that 0.1 g/L unlabeled L-histidine was added during cell growth: [U-^{15}N, NA-His]-IscR(WT). A third sample uniformly labeled with ^{15}N was prepared from the IscR variant in which both His143 and His145 were substituted with Ala: [U-^{15}N]-IscR(H143A, H145A). Following isolation and purification, these samples were concentrated under anaerobic conditions to 1.5 mM for NMR analysis.

^{15}N-NMR spectroscopy

A five-fold molar excess of sodium dithionite was added to reduce the samples. Protein samples were transferred to NMR tubes equipped with a J. Young valve (Wilmad, Vineland, NJ) under anaerobic conditions and then sealed. ^{15}N NMR spectra were collected on a Bruker 500 MHz NMR spectrometer. Short recycling delays were used to suppress signals from slowly relaxing nuclei distant from the cluster. The pH was measured before and after data collection and was found to be unchanged. Chemical shifts were referenced to sodium 2,2-dimethyl-2-silapentane-5-sulfonate (DSS). NMR data were collected at two temperatures (298 K and 288 K) to identify hyperfine shifted signals from their temperature dependence.

DNA binding fluorescence assays

IscR binding to double stranded DNA (dsDNA) containing the *iscR* binding site (-42 to -12 relative to the transcription start site) was measured using fluorescence polarization assays as described previously (5). The assays were performed under anaerobic conditions with and without added dithionite using wild type IscR from strain PK8581 that was isolated under anaerobic conditions as described previously (1) but exposed to O_2 for 5 min.

Results

Mössbauer studies of IscR as-purified and in whole cells

The 4.2 K Mössbauer spectra show that IscR is a mixture of oxidized and reduced states upon anaerobic isolation (data not shown). Therefore, as-isolated IscR was exposed to air to obtain the spectrum of the oxidized state (Figure 1), and the sample was subsequently reduced with dithionite to obtain the spectrum of the reduced state (Figure 2). The 4.2 K spectrum of oxidized IscR exhibits two overlapping quadrupole doublets in a 1:1 intensity ratio with quadrupole splittings and isomer shifts of $\Delta E_Q(1) = -0.48$ mm/s, $\delta(1) = 0.27$ mm/s and $\Delta E_Q(2) = +0.72$ mm/s, $\delta(2) = 0.30$ mm/s. These parameters are characteristic of $[2Fe\text{-}2S]^{2+}$ clusters. In their 2+ oxidation state $[2Fe\text{-}2S]^{2+}$ clusters possess a *diamagnetic* ground state, and this expectation is confirmed by the 8.0 T data of IscR (Figure 1B); thus the 8.0 T spectrum can be fitted by assuming the absence of ^{57}Fe magnetic hyperfine interactions. This spectrum also yields the asymmetry parameter (see below) of the electric field gradient (EFG) tensors, $\eta(1) = \eta(2) = 0.5$. The above assignment of the four lines assumes two nested doublets in Figure 1A; however, a non-nested assignment with $\Delta E_Q(1) = -0.57$ mm/s, $\delta(1) = 0.23$ mm/s and $\Delta E_Q(2) = +0.64$ mm/s, $\delta(2) = 0.34$ mm/s fits both spectra as well as the nested set.

Figure 2 shows 4.2 K Mössbauer spectra of dithionite reduced IscR recorded in parallel applied magnetic fields as indicated. These spectra have features typically observed for $[2Fe\text{-}2S]^{1+}$ clusters, and accordingly, we have analyzed them with a S = 1/2 spin Hamiltonian pertinent for the ground state of an antiferromagnetically coupled pair of high-spin Fe^{3+} (S = 5/2) and Fe^{2+} (S = 2), as described elsewhere.

$$\mathcal{H}=\beta S \bullet g \bullet B+\sum_{i=1,2} S \bullet A_i \bullet I - g_n\beta_n B \bullet I+\mathcal{H}_Q \quad (1)$$

with

$$\mathcal{H}_Q=\frac{eQV_{zz}}{12}\left[3I_z^2 - 15/4+\eta\left(I_x^2 - I_y^2\right)\right] \quad \text{and} \quad \eta=\left(V_{xx} - V_{yy}\right)/V_{zz}$$

In eqs (1) all symbols have their conventional meanings (17). The red solid lines in Figure 2 are spectral simulations using eq 1 with the parameters listed in Table 1. Since the **g**-tensor is rather isotropic, the orientation of the magnetic hyperfine tensors, $\mathbf{A}_i$, and the EFG tensors relative to **g** cannot be determined from a powder spectrum; for the simulations we have used $\mathbf{g} = g_{av} = 1.93$ according to the published EPR data (2) of IscR.

The dithionite-reduced protein contains a mononuclear high-spin Fe^{2+} contaminant accounting for 8% of the total Fe present. In small applied fields this contaminant exhibits a doublet with $\Delta E_Q = 3.35$ mm/s and $\delta = 0.70$ mm/s, indicated above the spectrum of Figure 2A. The isomer shift indicates a tetrahedral $Fe^{2+}(S)_3X$ (X = S, O, or N) site. We suspect that the contaminant represents [2Fe-2S] sites that lost one iron during incubation with dithionite.

The fits in Figure 2 reveal that the **A**-tensors of the ferric and ferrous sites have opposite signs, in accord with the standard spin coupling scheme used for $[2Fe\text{-}2S]^{1+}$ clusters, which predicts $\mathbf{A}(Fe^{3+}) = (7/3)\mathbf{a}(Fe^{3+})$ and $\mathbf{A}(Fe^{2+}) = (-4/3)\mathbf{a}(Fe^{3+})$, where the lower case quantities refer to the local **a**-tensors of the uncoupled sites. The isomer shift of the ferric site of the $[2Fe\text{-}2S]^{1+}$ cluster, $\delta = 0.33$ mm/s, coincides, within experimental error, with the $\delta(2)$ value of the oxidized cluster for the non-nested assignment. This observation, however, does not imply that the non-nested assignment for the oxidized, $[2Fe\text{-}2S]^{2+}$ cluster is correct, as the ferric sites of $[2Fe\text{-}2S]^{1+}$ clusters typically acquire some electron density by valence delocalization (double exchange) from the ferrous site. In fact, all ferric sites of reduced [2Fe-2S] clusters have δ-values that are larger than those observed in the oxidized state. For this reason, we prefer the nested assignment of the two doublets of the oxidized protein. In Table 1 we compare the hyperfine parameters of the reduced IscR protein with those reported for *Aquifex aeolicus* Fd1; for more detailed information, the reader is referred to Table 1 of Meyer et al. (18). Roughly speaking, the [2Fe-2S] ferredoxins divide into two classes on the basis of the orientation of the EFG of the ferrous site. For plant-type ferredoxins (e.g. the ferredoxins from spinach and parsley) the largest component of the EFG is negative and along *z*, reflecting a β electron in the $3d(z^2)$ orbital. In contrast, the largest EFG component of reduced IscR, like that of putidaredoxin, adrenodoxin, and *A. aeolicus* Fd1, is positive ($\eta < -1$) and along x. Analysis of the electronic structure of the reduced IscR protein is beyond the scope of the present study, but we wish to comment briefly on the δ-value of the ferrous site. The isomer shift of Fe^{2+} sites depends on the nature of the coordinated ligands, with $\delta(S) < \delta(N) < \delta(O)$. The isomer shifts of seven well studied proteins with cysteinyl coordination listed by Meyer et al. (18) range from 0.62 to 0.67 mm/s, with $\delta_{ave} = 0.65$ mm/s. The ferrous site of Rieske proteins has $\delta_{ave} = 0.73$ mm/s, reflecting coordination by nitrogens of two histidines. The δ-value of 0.70 mm/s of IscR is thus more consistent with His-Cys coordination. Moreover, we would expect that the His-coordinated site of IscR has the higher potential and is thus destined to be the reduced site in $[2Fe\text{-}2S]^{1+}$ IscR, as is indeed the case.

Mössbauer spectra of whole cells

Figure 3 shows 4.2 K Mössbauer spectra of whole *E. coli* cells. The spectrum in Figure 3A was obtained from cells lacking over-expressed IscR. Roughly 40% of the iron in this sample belongs to a collection of high-spin Fe^{2+} species with $\Delta E_Q \sim 3.0$ mm/s and $\delta \sim 1.3$ mm/s, outlined by the solid line. Most likely, these species represent octahedral Fe^{2+} sites with O and N coordination, as they lack features associated with iron-sulfur clusters or mononuclear FeS_4 sites. The central feature mostly represents high-spin Fe^{3+}, presumably belonging to aggregated iron. Aggregated ferric iron is indicated by broad magnetic features seen in a 5.0 T spectrum (not shown). The spectrum in Figure 3B was obtained from cells over-expressing wild type IscR. The low energy feature is readily recognized as belonging to an S = 1/2 $[2Fe\text{-}2S]^{1+}$ cluster, as observed with the purified protein. By subtracting from the spectrum of Figure 3B the spectrum of Figure 3A, and assuming that it represents 50% of total Fe in the cells over-expressing IscR, we obtained the spectrum in Figure 3C; the choice of 50% yields a spectrum whose outer features match those of the IscR $[2Fe\text{-}2S]^{1+}$. The red solid line is the theoretical curve for the purified protein (from Figure 2A), and it represents 32% of the Fe in the sample used to obtain the spectrum in Figure 3B. We do not know which species are contained in the central feature of Figure 3C that is not covered by the red line. We have considered whether it contains contributions from Fe-S clusters. First, if the sample used to obtain Figure 3B contained an oxidized IscR $[2Fe\text{-}2S]^{2+}$ cluster (there is no direct evidence), it could not represent more than 8% of the Fe. Second, we have no direct evidence for the presence of a $[4Fe\text{-}4S]^{2+}$ cluster; however, a spectrum recorded at 5.0 T (not shown), in which the absorption of much of the "aggregated" ferric iron is shifted to larger velocities, could accommodate a $[4Fe\text{-}4S]^{2+}$ cluster (but representing at most 10% of total Fe) with $\Delta E_Q = 1$ mm/s and $\delta = 0.45$ mm/s. Thus, in cells containing over-expressed IscR there are at least 6 times as many IscR $[2Fe\text{-}2S]^{1+}$ clusters as $[4Fe\text{-}4S]^{2+}$ clusters. Even if 10% of the Fe in the sample used to obtain Figure 3B did indeed belong to a $[4Fe\text{-}4S]^{2+}$ cluster, such a cluster could also belong to proteins other than IscR. Taken together, our data suggest that IscR ligates a [2Fe-2S] cluster *in vivo* and that this cluster is observed predominantly in the reduced state.

Resonance Raman data indicate partial non-cysteinyl ligation of the cluster to IscR

Anaerobically isolated [2Fe-2S]-IscR was also characterized by resonance Raman spectroscopy to investigate the cluster ligation scheme. In particular, resonance Raman spectra in the Fe-S stretching region (200-450 cm^{-1}) of Fe-S cluster-containing proteins can report on the ligation of the cluster (19-22). Therefore, the resonance Raman spectrum of [2Fe-2S]-IscR isolated under anaerobic conditions was collected using 488 nm excitation (Figure 4).

The spectrum of IscR is not consistent with $(Cys)_4$ ligation based on a comparison with spectra of well-characterized [2Fe-2S] ferredoxins (23, 24). The $b_{3u}{}^t$ mode with predominant Fe-S^t stretching character occurs in the range of 281-292 cm^{-1} (one broad band) in spectra of these ferredoxins with $(Cys)_4$ ligation. This band is upshifted in the spectra of proteins that ligate [2Fe-2S] clusters via three cysteines and either one serine or one aspartate (20-22). For example, the $b_{3u}{}^t$ mode is upshifted from 292 cm^{-1} to 302 cm^{-1} upon substitution of a coordinating cysteine ligand with serine in the [2Fe-2S]-ferredoxin of *Clostridium pasteurianum* (21). Therefore, the presence of a band at 302 cm^{-1} in the spectrum of IscR could suggest $(Cys)_3(O)_1$ ligation of the cluster.

However, the presence of a band at 267 cm^{-1} in conjunction with a band at 302 cm^{-1} in the spectrum of IscR suggests that the unidentified fourth ligand could be a histidine. The spectra of Rieske-type [2Fe-2S] clusters with $(Cys)_2(His)_2$ ligation display two peaks in this low-frequency region that are sensitive to perturbations to the Fe-His bonding interactions

(25). For example, the archaeal Rieske-type ferredoxin of *Sulfolobus solfataricus* spectrum exhibits peaks at 260 cm^{-1} and 310 cm^{-1} that are downshifted to 258 cm^{-1} and 304 cm^{-1} upon substitution of one cluster-ligating histidine with cysteine to create $(Cys)_3(His)_1$ ligation (26). Similar to the spectra of Rieske clusters, the resonance Raman spectra of both the $(Cys)_3(His)_1$-coordinated [2Fe-2S]-Fra2-Grx3 (275 cm^{-1} and 300 cm^{-1}) (10) and the structurally characterized $(Cys)_3(His)_1$-coordinated [2Fe-2S]-mitoNEET (~265 cm^{-1} and ~295 cm^{-1}) (27) exhibit two bands in the 250-320 cm^{-1} region that suggest partial histidyl ligation. In contrast, the substitution of the histidine ligand of mitoNEET with cysteine, creating $(Cys)_4$ ligation, results in the appearance of only a single band at ~280 cm^{-1} in the resonance Raman spectrum, consistent with the spectra of other [2Fe-2S] clusters ligated by four cysteines (10, 27).

Therefore, the resonance Raman spectrum of [2Fe-2S]-IscR is consistent with coordination of the [2Fe-2S] cluster by three cysteines and one other ligand that ligates the cluster via an O or N atom. The resonance Raman spectrum of D_2O-exchanged IscR was nearly identical to that of the protein before exchange (data not shown), ruling out the possibility of a cluster-ligating bridging water/hydroxide molecule. Therefore, mutagenesis studies were performed to identify the amino acid side chain necessary for cluster ligation.

His107 is essential for cluster ligation to IscR

Since collectively the Mössbauer and resonance Raman data suggested that the [2Fe-2S] cluster is coordinated via an O or N atom, we substituted with alanine mostly conserved amino acids that could potentially ligate the cluster via an O or N atom. The targeted amino acids included several highly conserved residues near the cysteine-rich region of IscR (Tyr65, Asp84, Glu85, Thr106, His107, and Trp110), the Glu43 residue in the DNA binding domain that has been proposed to be the fourth ligand to the IscR cluster in *A. ferrooxidans* (28), and the other histidines of IscR, His143 and His145. If any of these residues acted as the fourth cluster ligand, we would expect that an alanine substitution at that position would remove an O or N bond to the cluster. Hence, such a substitution should result in a protein variant that most likely would lack an Fe-S cluster upon isolation and would be defective in repressing the *iscR* promoter.

IscR variants were tested for their ability to repress the *iscR* promoter under anaerobic growth conditions as an indication of the ability of the variants to ligate an Fe-S cluster *in vivo*. In contrast to the strain expressing wild type IscR, P_{iscR}-*lacZ* was not repressed under anaerobic growth conditions in a strain containing IscR with alanine substitutions of all three cluster-coordinating cysteines (the triple mutant, IscR-C92A/C98A/C104A), consistent with cluster ligation by IscR being required for repression of the *iscR* promoter. Of the other variants tested, only IscR-H107A displayed the same defective phenotype as IscR-C92A/C98A/C104A (Figure 5A and data not shown). Importantly, the lack of repression by IscR-(C92A/C98A/C104A) and IscR-H107A was not due to any substantial decrease in protein levels compared to wild type levels, as determined by Western blot analysis (data not shown). The lack of activity of IscRH107A *in vivo* was correlated with the lack of the Fe-S cluster *in vitro*, since isolation of IscRH107A under anaerobic conditions yielded apo-protein (Figure 5B). In contrast, wild type IscR, IscR-E43A, and the double mutant IscR-H143A/H145A, for example, were occupied with cluster when isolated under the same anaerobic conditions. These results suggest that His107 is important for cluster binding to IscR.

The effect of substituting His107 with cysteine, to potentially create a $(Cys)_4$ ligated cluster, was also tested. Partial repression of P_{iscR}-*lacZ* was observed when the strain containing IscR-H107C was tested under anaerobic growth conditions, suggesting some Fe-S cluster coordination *in vivo* (Figure 5A). Despite some activity *in vivo*, there was no detectable

[2Fe-2S] cluster in anaerobically isolated IscR-H107C (Figure 5B). Since activity *in vivo* reflects both synthesis and turnover, a mutant with reduced cluster stability can still demonstrate activity, if the synthesis rate is greater than cluster turnover. However, isolated protein only reflects the lability of the cluster. Thus, the cluster of the variant protein is not as stable as the cluster present in wild type IscR. Cluster instability has previously been observed in Fra2-Grx3 upon substitution of the histidine cluster ligand with cysteine, likely due to lengthening of the Fe-Fe distance and the original Fe-S bond distances (11). However, the observation that cysteine can partially substitute for histidine in IscR is consistent with the imidazole ring of His107 being structurally poised to act as a direct cluster ligand.

^{15}N-NMR supports hypothesis that His107 is a cluster ligand in [2Fe-2S]-IscR

^{15}N-NMR spectra were collected with rapid recycling times from three samples of reduced holoprotein at pH 6.4 and 298 K: [U-^{15}N]-IscR(WT) (Figure 6A), [U-^{15}N]-IscR(H143A, H145A) (Figure 7B), and [U-^{15}N]-IscR(U-^{15}N, NA-His) (Figure 6C). Comparison of these spectra identified two ^{15}N peaks arising from rapidly relaxing histidine residues and further identified one of these signals as arising from His107. Because of the lower protein concentration of [U-^{15}N]-IscR(H143A, H145A), the sensitivity was insufficient to resolve the second signal in the spectrum of this sample (Figure 6B); however, the second signal was observed in spectra collected at higher temperature. These results allowed us to assign the two ^{15}N peaks to His107. Comparison of ^{15}N NMR spectra of [U-^{15}N]-IscR(WT) collected at 298 K (Figure 7A) and 288 K (Figure 7B) showed that the two peaks assigned to His107 shifted to higher frequency with increasing temperature. Comparison of ^{15}N NMR spectra of [U-^{15}N]-IscR(WT) collected at two different delays between acquisition pulses (1.0 s and 5.0 ms) confirmed that the signals assigned to His107 relax rapidly, as expected for an Fe-S cluster ligand. We investigated the pH dependence of the two ^{15}N signals assigned to His107 and found that the signal at higher frequency exhibited a larger titration shift than that at lower frequency (Figure 8A). Each signal shifted continuously with pH, indicating rapid proton exchange between the two protonation states. Both signals were observed to sharpen in the protonated state at low pH.

Cluster oxidation state does not influence the DNA binding properties of holo-IscR

As discerned from Mössbauer spectroscopy, the cluster of IscR is primarily in the reduced form *in vivo* and is partially oxidized upon anaerobic isolation of the protein. In addition, previous studies of the [2Fe-2S] cluster of anaerobically isolated IscR illustrate that the cluster can be oxidized by O_2 and reversibly reduced/oxidized without significant decomposition (2). Therefore, by comparing the affinity of O_2-exposed IscR for dsDNA containing the *iscR* site in the absence and presence of dithionite, we can explore whether the oxidation state of the cluster affects the ability of IscR to bind to the *iscR* promoter. *In vitro* DNA binding assays illustrate that air-oxidized IscR (containing predominantly [2Fe-2S]$^{2+}$) bound to dsDNA containing the *iscR* binding site with similar affinity as dithionite-reduced IscR containing predominantly [2Fe-2S]$^{1+}$ (Figure 9). Therefore, oxidation of the cluster of IscR from [2Fe-2S]$^{1+}$ to [2Fe-2S]$^{2+}$ does not appear to affect DNA binding properties.

Discussion

IscR is a global regulator involved in a homeostatic mechanism controlling Fe-S cluster biogenesis and is proposed to act as a sensor of the cellular demands for Fe-S cluster biogenesis. The mechanism by which IscR senses the demand has not yet been detailed, but we expect that the Fe-S cluster of IscR has some unusual features that are relevant to this function. Indeed, the data presented here suggest that IscR of *E. coli* contains a reduced

$[2Fe\text{-}2S]^{1+}$ cluster *in vivo* with $(Cys)_3(His)_1$ ligation, which is a fairly uncommon ligation scheme.

All of the spectroscopic data are consistent with $(Cys)_3(His)_1$ ligation. The ^{15}N NMR data were particularly informative in assigning His107 to a likely role in cluster ligation. The two signals assigned to His107 decreased in intensity upon oxidation of the protein (data not shown) indicating that their chemical shifts are highly dependent on the redox state. The two ^{15}N signals exhibited rapid relaxation and anti-Curie temperature dependence (i.e., increasing paramagnetic shifts with decreasing temperature), as expected for a ligand bound to an antiferromagnetically coupled cluster. Both signals exhibited pH titration shifts of the type observed for His imidazole ring nitrogens ($^{15}N^{\delta 1}$ and $^{15}N^{\epsilon 2}$) ligated to a [2Fe-2S] cluster in a Rieske protein (29, 30). In Rieske proteins, however, ^{15}N signals were unable to be resolved from ring nitrogens ligated to the iron (29-31) presumably because they were too broad to be detected. We suspect that the broader peak at higher frequency (Figures 7-9) corresponds to the nitrogen atom ligated to Fe. The fact that this signal is observed suggests that the degree of unpaired electron spin delocalization onto this atom is lower in a $(Cys)_3(His)_1$-ligated Fe-S protein than in a $(Cys)_2(His)_2$-ligated Rieske protein. The sharpening of the ^{15}N NMR signals at low pH indicates that the addition of a positively charged proton to the ligand His decreases its interaction with the positively-charged cluster.

Interestingly, the number of proteins currently identified as binding a [2Fe-2S] cluster with $(Cys)_3(His)_1$ ligation appear to have possible roles as sensors. IscR directly regulates the transcription of the *isc* operon, which encodes the proteins that constitute the primary pathway of Fe-S cluster biogenesis in *E. coli* (2). Further, the role of IscR has been expanded to include a role as a global regulator that senses and responds to the cellular demand for cluster synthesis and/or repair (1, 5). The yeast proteins Fra2 and Grx3 are involved in sensing the cellular iron status and subsequently transmitting a signal to the transcriptional activators Aft1 and Aft2 (32-34). Although the mechanism has not been elucidated, Aft1/2 activity is inhibited under iron-replete conditions via interactions with the Fra2 and Grx3 proteins that promote the export of Aft1/2 from the nucleus. Lastly, the function of the mitochondrial protein mitoNEET is not as well defined as those of the proteins discussed here. However, the [2Fe-2S] cluster of mitoNEET, which is not stable *in vitro* below pH 8 (35), is stabilized by the binding of the thiazolidinedione class of anti-diabetes drugs (36, 37). As this class of drugs is known to enhance oxidative capacity, ligation of an Fe-S cluster to mitoNEET may allow it to act as a sensor of oxidative stress or, perhaps due to the intimate link between the two (38), the cellular iron status. Whether or not a sensor function will be assigned to other, yet to be identified, proteins that bind [2Fe-2S] clusters with $(Cys)_3(His)_1$ ligation remains to be seen.

It is also of interest to consider the ligation of Fe-S clusters to other transcription factors with sensor functions as we attempt to understand the cluster and protein features that define sensor function. An example of note is the NO sensor NsrR, which is a member of the Rrf2 family of transcription factors that includes IscR. While the three cysteines are conserved between IscR and NsrR, His107 is not conserved (9). Rather, the residue corresponding to His107 in *E. coli* NsrR is lysine, and preliminary data suggest that *E. coli* IscR-H107K is in the apo-form upon anaerobic isolation. Whether or not the apparent difference in cluster ligands between IscR, a sensor of Fe-S cluster demand, and NsrR, a sensor of NO, is related to their differing sensor functions remains to be seen.

The recognition of an atypical ligation scheme for the [2Fe-2S] cluster of IscR does, however, provide some new insight for investigating possible sensing mechanisms. The feedback model of IscR repression proposes that IscR acquires an Fe-S cluster via the Isc proteins once the cellular demand for Fe-S cluster biogenesis is satisfied (2), suggesting that

the Isc proteins might be able to distinguish between IscR and other apo-protein targets. While the details of target specificity of the Isc proteins remain elusive (39), the proposed $(Cys)_3(His)_1$ ligation scheme of IscR could differentiate it from other apo-proteins. Perhaps by making IscR a poor substrate for the Isc proteins via one atypical amino acid ligand, IscR is able to sense the cellular demand for Fe-S cluster biogenesis indirectly by the availability of the Isc machinery to associate with IscR.

The ligation scheme observed for IscR does not appear to confer any unusual sensitivity to O_2 that could make the Fe-S cluster occupancy of IscR sensitive to the general cellular demands for Fe-S cluster biogenesis. *In vivo*, [2Fe-2S]-IscR regulates the *iscR* promoter and appears to be mostly in the reduced state under anaerobic growth conditions. However, changes in the cluster oxidation state upon exposure to O_2 do not alter the ability of IscR to bind to the *iscR* site *in vitro*, suggesting that changes in cluster oxidation state may not be relevant to the sensor function of IscR. Therefore, IscR may not directly respond to O_2, and the functional relevance of the ability of [2Fe-2S]-IscR to be reversibly oxidized and reduced is not clear. However, the data do not preclude the possibility that the proposed $(Cys)_3(His)_1$ cluster ligation scheme makes IscR more prone to cluster loss upon prolonged exposure to O_2 or reactive oxygen species, which will be addressed in further studies.

The identification of His107 as a likely cluster ligand in IscR of *E. coli* also has implications for the structure-function relationship of IscR. As IscR function is linked to cluster binding, interactions between the DNA-binding domain and cluster-binding domain are likely essential for IscR function. The proposal that Glu43, a residue in the predicted DNA binding domain, acts as the fourth ligand to the cluster in IscR of *A. ferrooxidans* (28) suggested a direct mechanism for the communication of cluster acquisition (or loss) between the two domains. However, based on the recent X-ray crystal structure of *Bacillus subtilis* CymR, a member of the Rrf2 family of transcription factors, Glu43 (Glu44 in CymR) is expected to make direct contacts to the DNA site and thus does not appear to be structurally poised to act as a cluster ligand (40). Therefore, communication of cluster acquisition (or loss) to the DNA binding domain is more likely to occur via interactions between residues in the cluster-binding region of one monomer and residues in the DNA binding region of the other monomer of the IscR homodimer, similar to what was observed in the X-ray crystal structure of the transcription factor $[2Fe\text{-}2S]^{2+}$-SoxR of *E. coli* (41). The conformational changes that occur upon cluster binding to IscR are not yet known.

References

1. Giel JL, Rodionov D, Liu MZ, Blattner FR, Kiley PJ. IscR-dependent gene expression links iron-sulphur cluster assembly to the control of O_2-regulated genes in *Escherichia coli*. Mol. Microbiol. 2006; 60:1058–1075. [PubMed: 16677314]
2. Schwartz CJ, Giel JL, Patschkowski T, Luther C, Ruzicka FJ, Beinert H, Kiley PJ. IscR, an Fe-S cluster-containing transcription factor, represses expression of *Escherichia coli* genes encoding Fe-S cluster assembly proteins. Proc. Natl. Acad. Sci. U. S. A. 2001; 98:14895–14900. [PubMed: 11742080]
3. Frazzon J, Dean DR. Feedback regulation of iron-sulfur cluster biosynthesis. Proc. Natl. Acad. Sci. U. S. A. 2001; 98:14751–14753. [PubMed: 11752417]
4. Yeo WS, Lee JH, Lee KC, Roe JH. IscR acts as an activator in response to oxidative stress for the *suf* operon encoding Fe-S assembly proteins. Mol. Microbiol. 2006; 61:206–218. [PubMed: 16824106]
5. Nesbit AD, Giel JL, Rose JC, Kiley PJ. Sequence-specific binding to a subset of IscR-regulated promoters does not require IscR Fe-S cluster ligation. J. Mol. Biol. 2009; 387:28–41. [PubMed: 19361432]
6. Guigliarelli B, Bertrand P. Application of EPR spectroscopy to the structural and functional study of iron-sulfur proteins. Adv. Inorg. Chem. 1999; 47:421–497.

7. Orio M, Mouesca JM. Variation of average *g* values and effective exchange coupling constants among [2Fe-2S] clusters: a density functional theory study of the impact of localization (trapping forces) versus delocalization (double-exchange) as competing factors. Inorg. Chem. 2008; 47:5394–5416. [PubMed: 18491857]
8. Finn RD, Mistry J, Tate J, Coggill P, Heger A, Pollington JE, Gavin OL, Gunasekaran P, Ceric G, Forslund K, Holm L, Sonnhammer ELL, Eddy SR, Bateman A. The Pfam protein families database. Nucleic Acids Res. 2010; 38:D211–D222. [PubMed: 19920124]
9. Tucker NP, Le Brun NE, Dixon R, Hutchings MI. There's NO stopping NsrR, a global regulator of the bacterial NO stress response. Trends Microbiol. 2010; 18:149–156. [PubMed: 20167493]
10. Li HR, Mapolelo DT, Dingra NN, Naik SG, Lees NS, Hoffman BM, Riggs-Gelasco PJ, Huynh BH, Johnson MK, Outten CE. The yeast iron regulatory proteins Grx3/4 and Fra2 form heterodimeric complexes containing a [2Fe-2S] cluster with cysteinyl and histidyl ligation. Biochemistry. 2009; 48:9569–9581. [PubMed: 19715344]
11. Li HR, Mapolelo DT, Dingra NN, Keller G, Riggs-Gelasco PJ, Winge DR, Johnson MK, Outten CE. Histidine-103 in Fra2 is an iron-sulfur cluster ligand in the [2Fe-2S] Fra2-Grx3 complex and is required for *in vivo* iron signaling in yeast. J. Biol. Chem. 2011; 286:867–876. [PubMed: 20978135]
12. Yan AX, Kiley PJ. Techniques to isolate O_2-sensitive proteins: [4Fe-4S]-FNR as an example. Meth. Enzymol. 2009; 463:787–805. [PubMed: 19892202]
13. Khoroshilova N, Popescu C, Munck E, Beinert H, Kiley PJ. Iron-sulfur cluster disassembly in the FNR protein of *Escherichia coli* by O_2: 4Fe-4S to 2Fe-2S conversion with loss of biological activity. Proc. Natl. Acad. Sci. U. S. A. 1997; 94:6087–6092. [PubMed: 9177174]
14. Popescu CV, Bates DM, Beinert H, Münck E, Kiley PJ. Mössbauer spectroscopy as a tool for the study of activation/inactivation of the transcription regulator FNR in whole cells of *Escherichia coli*. Proc. Natl. Acad. Sci. U. S. A. 1998; 95:13431–13435. [PubMed: 9811817]
15. Sutton VR, Stubna A, Patschkowski T, Münck E, Beinert H, Kiley PJ. Superoxide destroys the $[2Fe\text{-}2S]^{2+}$ cluster of FNR from *Escherichia coli*. Biochemistry. 2004; 43:791–798. [PubMed: 14730984]
16. Miller, JH. Experiments in Molecular Genetics. Cold Spring Harbor Laboratory Press; Plainview, NY: 1972.
17. Münck E. Mössbauer spectroscopy of proteins: electron carriers. Meth. Enzymol. 1978; 54:346–379. [PubMed: 215877]
18. Meyer J, Clay MD, Johnson MK, Stubna A, Munck E, Higgins C, Wittung-Stafshede P. A hyperthermophilic plant-type 2Fe-2S ferredoxin from *Aquifex aeolicus* is stabilized by a disulfide bond. Biochemistry. 2002; 41:3096–3108. [PubMed: 11863449]
19. Kuila D, Schoonover JR, Dyer RB, Batie CJ, Ballou DP, Fee JA, Woodruff WH. Resonance Raman studies of Rieske-type proteins. Biochim. Biophys. Acta. 1992; 1140:175–183. [PubMed: 1280165]
20. Crouse BR, Sellers VM, Finnegan MG, Dailey HA, Johnson MK. Site-directed mutagenesis and spectroscopic characterization of human ferrochelatase: identification of residues coordinating the [2Fe-2S] cluster. Biochemistry. 1996; 35:16222–16229. [PubMed: 8973195]
21. Meyer J, Fujinaga J, Gaillard J, Lutz M. Mutated forms of the [2Fe-2S] ferredoxin from *Clostridium pasteurianum* with noncysteinyl ligands to the iron-sulfur cluster. Biochemistry. 1994; 33:13642–13650. [PubMed: 7947772]
22. Duin EC, Lafferty ME, Crouse BR, Allen RM, Sanyal I, Flint DH, Johnson MK. [2Fe-2S] to [4Fe-4S] cluster conversion in *Escherichia coli* biotin synthase. Biochemistry. 1997; 36:11811–11820. [PubMed: 9305972]
23. Han S, Czernuszewicz RS, Kimura T, Adams MWW, Spiro TG. Fe_2S_2 protein resonance Raman-spectra revisited: structural variations among adrenodoxin, ferredoxin, and red paramagnetic protein. J. Am. Chem. Soc. 1989; 111:3505–3511.
24. Fu WG, Drozdzewski PM, Davies MD, Sligar SG, Johnson MK. Resonance Raman and magnetic circular dichroism studies of reduced [2Fe-2S] proteins. J. Biol. Chem. 1992; 267:15502–15510. [PubMed: 1639790]

25. Rotsaert FAJ, Pikus JD, Fox BG, Markley JL, Sanders-Loehr J. N-isotope effects on the Raman spectra of Fe_2S_2 ferredoxin and Rieske ferredoxin: evidence for structural rigidity of metal sites. J. Biol. Inorg. Chem. 2003; 8:318–326. [PubMed: 12589567]
26. Kounosu A, Li ZR, Cosper NJ, Shokes JE, Scott RA, Imai T, Urushiyama A, Iwasaki T. Engineering a three-cysteine, one-histidine ligand environment into a new hyperthermophilic archaeal Rieske-type [2Fe-2S] ferredoxin from *Sulfolobus solfataricus*. J. Biol. Chem. 2004; 279:12519–12528. [PubMed: 14726526]
27. Tirrell TF, Paddock ML, Conlan AR, Smoll EJ, Nechushtai R, Jennings PA, Kim JE. Resonance Raman studies of the $(His)(Cys)_3$ 2Fe-2S Cluster of mitoNEET: comparison to the $(Cys)_4$ mutant and implications of the effects of pH on the labile metal center. Biochemistry. 2009; 48:4747–4752. [PubMed: 19388667]
28. Zeng J, Zhang XJ, Wang YP, Ai CB, Liu Q, Qiu GZ. Glu43 is an essential residue for coordinating the $[Fe_2S_2]$ cluster of IscR from *Acidithiobacillus ferrooxidans*. FEBS Lett. 2008; 582:3889–3892. [PubMed: 18955052]
29. Lin I-J, Chen Y, Fee JA, Song JK, Westler WM, Markley JL. Rieske protein from *Thermus thermophilus*: ^{15}N NMR titration study demonstrates the role of iron-ligated histidines in the pH dependence of the reduction potential. J. Am. Chem. Soc. 2006; 128:10672–10673. [PubMed: 16910649]
30. Hsueh K-L, Westler WM, Markley JL. NMR investigation of the Rieske protein from *Thermus thermophilus* support a coupled proton and electron transfer mechanism. J. Am. Chem. Soc. 2010; 132:7908–7918. [PubMed: 20496909]
31. Xia B, Pikus JD, Xia WD, McClay K, Steffan RJ, Chae YK, Westler WM, Markley JL, Fox BG. Detection and classification of hyperfine-shifted ^1H, ^2H, and ^{15}N resonances of the Rieske ferredoxin component of toluene 4-monooxygenase. Biochemistry. 1999; 38:727–739. [PubMed: 9888813]
32. Kumanovics A, Chen OS, Li LT, Bagley D, Adkins EM, Lin HL, Dingra NN, Outten CE, Keller G, Winge D, Ward DM, Kaplan J. Identification of FRA1 and FRA2 as genes involved in regulating the yeast iron regulon in response to decreased mitochondrial iron-sulfur cluster synthesis. J. Biol. Chem. 2008; 283:10276–10286. [PubMed: 18281282]
33. Ojeda L, Keller G, Muhlenhoff U, Rutherford JC, Lill R, Winge DR. Role of glutaredoxin-3 and glutaredoxin-4 in the iron regulation of the Aft1 transcriptional activator in *Saccharomyces cerevisiae*. J. Biol. Chem. 2006; 281:17661–17669. [PubMed: 16648636]
34. Pujol-Carrion N, Belli G, Herrero E, Nogues A, de la Torre-Ruiz MA. Glutaredoxins Grx3 and Grx4 regulate nuclear localisation of Aft1 and the oxidative stress response in *Saccharomyces cerevisiae*. J. Cell Sci. 2006; 119:4554–4564. [PubMed: 17074835]
35. Wiley SE, Paddock ML, Abresch EC, Gross L, van der Geer P, Nechushtai R, Murphy AN, Jennings PA, Dixon JE. The outer mitochondrial membrane protein mitoNEET contains a novel redox-active 2Fe-2S cluster. J. Biol. Chem. 2007; 282:23745–23749. [PubMed: 17584744]
36. Paddock ML, Wiley SE, Axelrod HL, Cohen AE, Roy M, Abresch EC, Capraro D, Murphy AN, Nechushtai R, Dixon JE, Jennings PA. MitoNEET is a uniquely folded 2Fe-2S outer mitochondrial membrane protein stabilized by pioglitazone. Proc. Natl. Acad. Sci. U. S. A. 2007; 104:14342–14347. [PubMed: 17766440]
37. Bak DW, Zuris JA, Paddock ML, Jennings PA, Elliott SJ. Redox characterization of the FeS protein mitoNEET and impact of thiazolidinedione drug binding. Biochemistry. 2009; 48:10193–10195. [PubMed: 19791753]
38. Imlay JA. Cellular defenses against superoxide and hydrogen peroxide. Annu. Rev. Biochem. 2008; 77:755–776. [PubMed: 18173371]
39. Ayala-Castro C, Saini A, Outten FW. Fe-S cluster assembly pathways in bacteria. Microbiol. Mol. Biol. Rev. 2008; 72:110–125. [PubMed: 18322036]
40. Shepard W, Soutourina O, Courtois E, England P, Haouz A, Martin-Verstraete I. Insights into the Rrf2 repressor family: the structure of CymR, the global cysteine regulator of Bacillus subtilis. FEBS J. 2011; 278:2689–2701. [PubMed: 21624051]

41. Watanabe S, Kita A, Kobayashi K, Miki K. Crystal structure of the [2Fe-2S] oxidative-stress sensor SoxR bound to DNA. Proc. Natl. Acad. Sci. U. S. A. 2008; 105:4121–4126. [PubMed: 18334645]

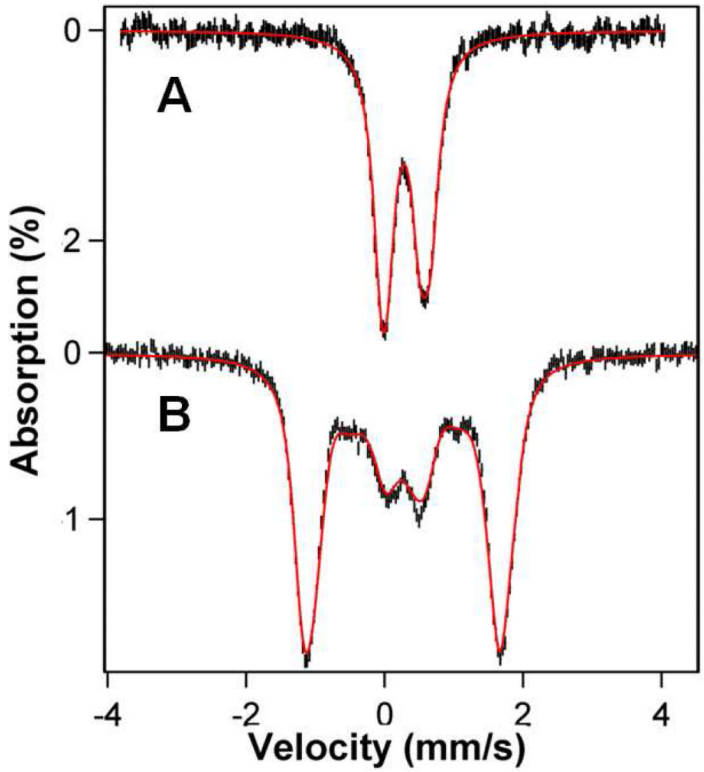

Figure 1.

4.2 K Mössbauer spectra of anaerobically isolated IscR that has been exposed to air recorded in zero field (A) and for B = 8.0 T (B). Solid lines are simulations assuming a cluster with S = 0 using the nested set of parameters: $\Delta E_Q(1)$ = -0.48 mm/s, $\delta(1)$ = 0.27 mm/s, $\eta(1)$ = 0.5; $\Delta E_Q(2)$ = +0.72 mm/s, $\delta(2)$ = 0.30 mm/s, $\eta(2)$ = 0.5.

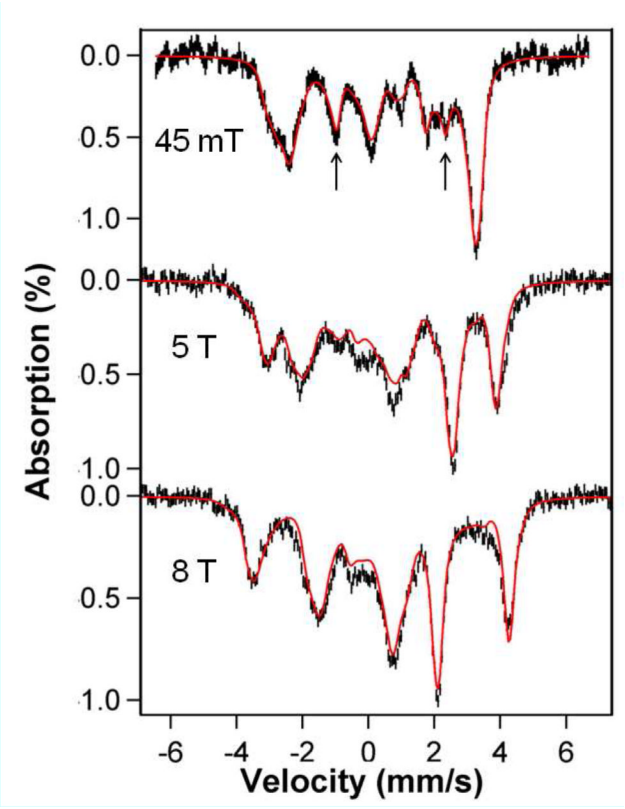

Figure 2.

4.2 K Mössbauer spectra of dithionite reduced IscR recorded in parallel applied field as indicated. The solid red lines are a spectral simulation based on eq 1 using the parameters listed in Table 1. For the simulation of the 45 mT spectrum we have added a doublet for a minor contaminant (8%, arrows) with ΔE_Q = 3.35 mm/s and δ = 0.70 mm/s.

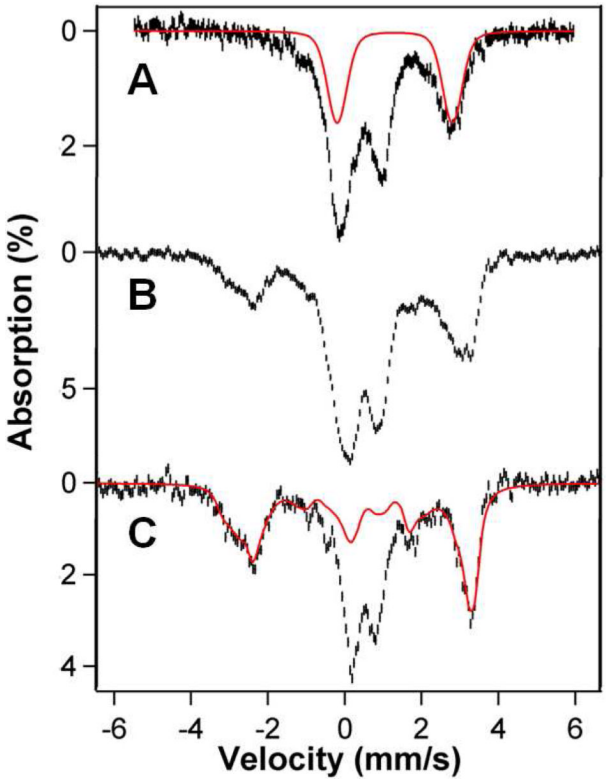

Figure 3.

Mössbauer spectra of whole cells recorded at 4.2 K in parallel applied fields on 45 mT. (A) Spectrum of whole *E. coli* cells without overexpression of IscR. Solid red line outlines contribution of a collection of high-spin Fe^{2+} species. (B) Spectrum of whole cells overexpressing wild type IscR. (C) Spectrum obtained by subtracting from (B) the spectrum of (A), assuming that it represents 50% of the Fe in sample. The procedure gives a good view of the features of the IscR cluster. The red line is the spectral simulation (representing 32% of Fe) from Figure 2 A (without the 8% contaminant).

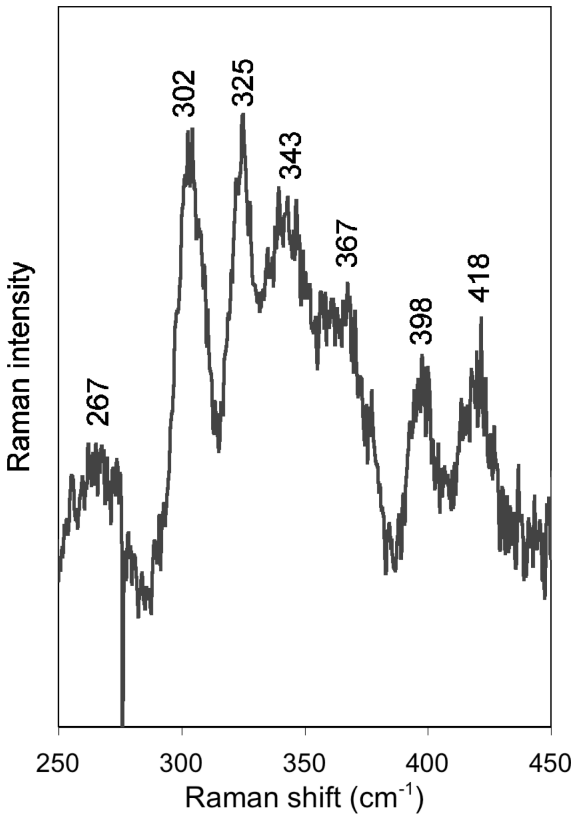

Figure 4.

77 K resonance Raman spectrum of anaerobically isolated IscR (47% occupancy, ~3 mM), obtained with laser excitation at 488 nm and a power of 100 mW at the sample (resolution is ~6 cm^{-1}). The average of nine scans is presented here, and the contributions from ice lattice vibrations were removed by subtracting a properly scaled spectrum of buffer obtained under identical conditions.

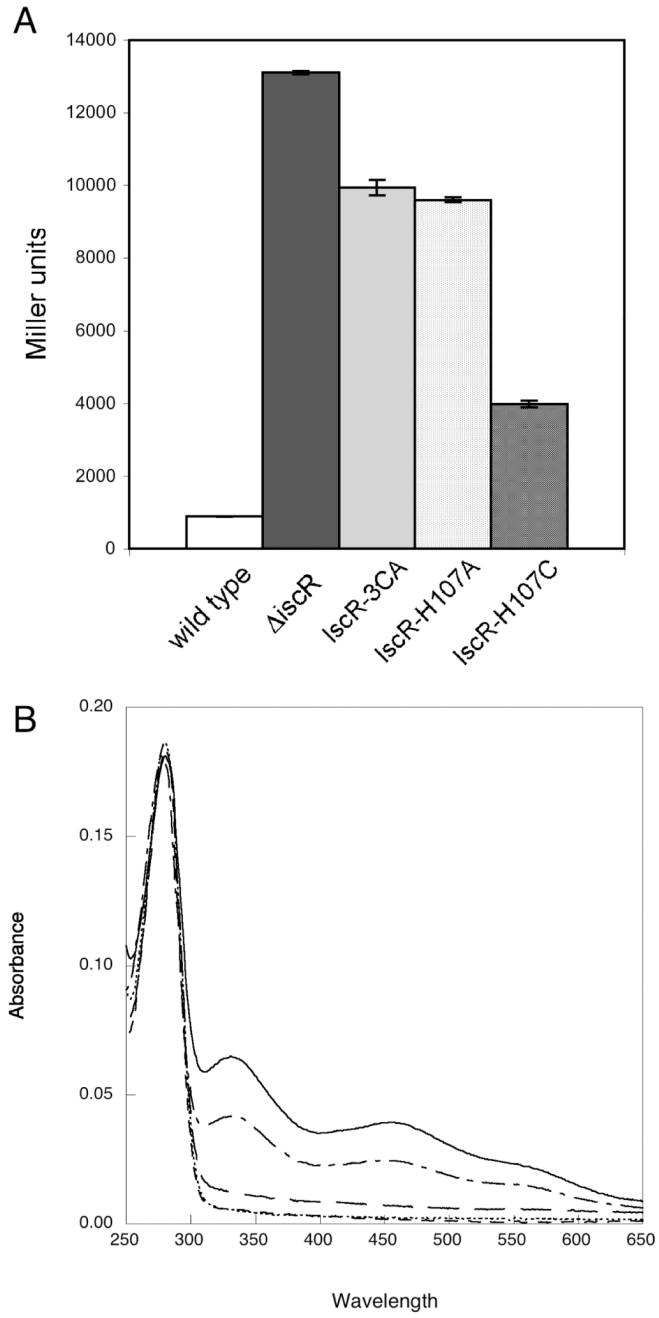

Figure 5.

(A) Expression levels of the *iscR* promoter fused to *lacZ* were determined in strains containing wild type IscR (white bar), Δ*iscR* (black bar), IscR-C92A/C98A/C104 (IscR-3CA, gray bar), IscR-H107A (light patterned bar), or IscR-H107C (dark patterned bar). Strains were grown under anaerobic conditions in MOPS minimal media containing 0.2% glucose and were assayed for β-galactosidase activity per OD_{600} (Miller units). (B) Optical spectra of IscR variants. The spectra of wild type IscR (solid line), IscR-E43A (— - —), IscR-C92A/C98A/C104A (— —), IscR-H107A (- - -), and IscR-H107C (· · ·) were obtained under anaerobic conditions in 10 mM HEPES, pH 7.4, with 200 mM KCl at room

temperature (10 μM protein). All variants were isolated under anaerobic conditions as described in the Methods.

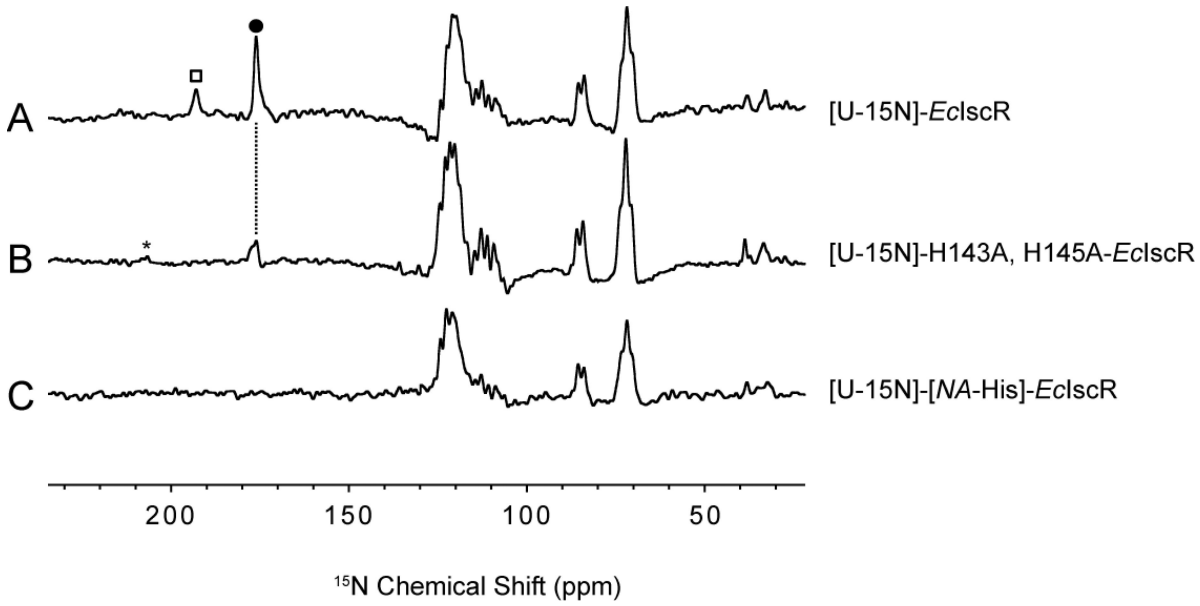

Figure 6.

^{15}N-NMR spectra of ~2 mM reduced IscR samples at pH 6.4 collected at 298 K under rapid pulsing conditions. (A) [U-^{15}N]-IscR(WT) produced from cells grown on $^{15}NH_4Cl$ as the sole nitrogen source. (B) [U-^{15}N]-IscR(H143A, H145A) produced from cells grown on $^{15}NH_4Cl$ as the sole nitrogen source. (C) [U-^{15}N]-IscR(WT) produced from cells grown on $^{15}NH_4Cl$ in the presence of unlabeled L-histidine. Together, these spectra show that the indicated signals (□ and •) in (A) arise from histidine residues and that the signal labeled with a closed dot (•) is from His107, the one His residue not removed by substitution in the sample whose spectrum is shown in (B). The peak labeled with an open square (□) appeared in other spectra of [U-^{15}N]-IscR(H143A, H145A), not shown. The peak labeled with an asterisk (*) is from $^{14}N^{15}N$ in nitrogen gas in air.

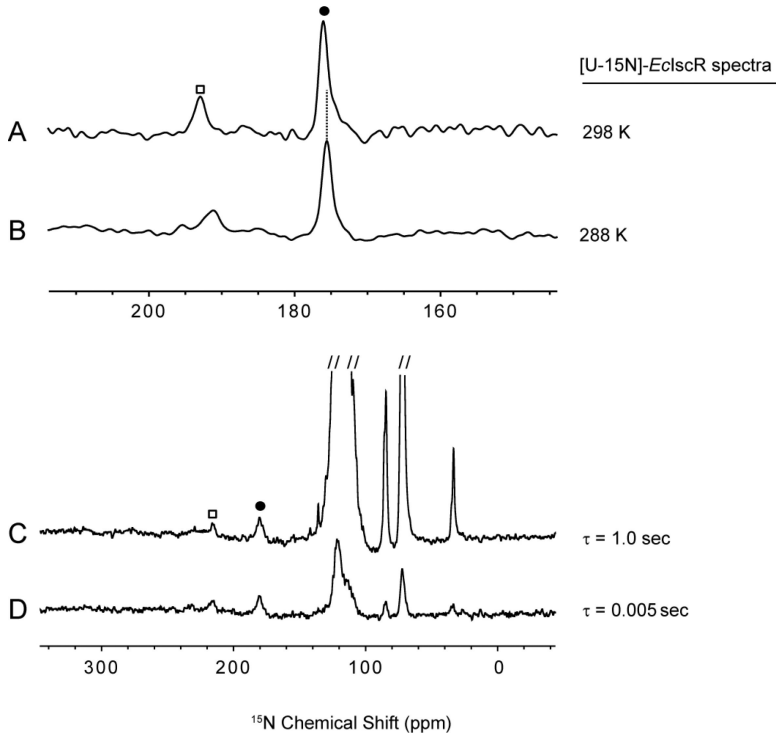

Figure 7.

Evidence from ^{15}N NMR spectra that the labeled signals (□ and •) of reduced [U-^{15}N]-IscR(WT) arise from nuclei affected by electron-nuclear (hyperfine) interactions. (A, B) The chemical shifts of the labeled peaks exhibit anti-Curie shifts as a function of temperature as expected for an Fe-S cluster ligand (delay value 5.0 ms). (C, D) Spectra taken as two different delay values (1.0 s and 5.0 ms) between the data collection pulses suggest that the labeled peaks correspond to rapidly relaxing nuclei as expected for a cluster ligand.

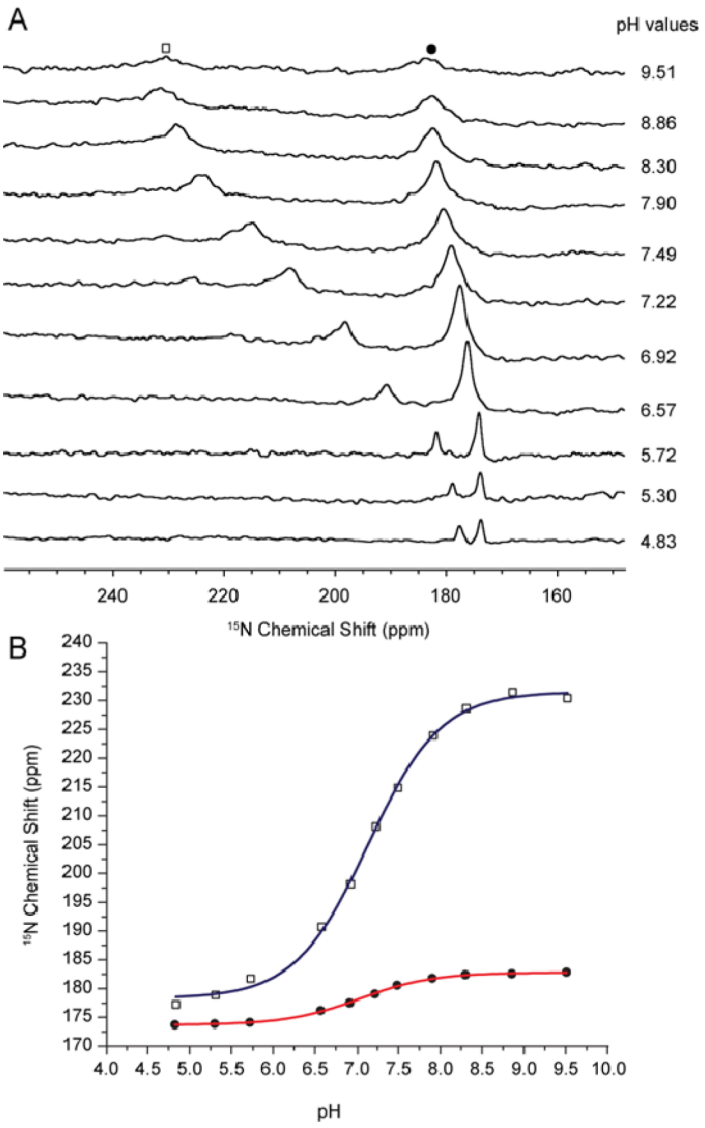

Figure 8.

(A) Dependence of ^{15}N NMR spectra of 2 mM reduced [U-^{15}N]-IscR(WT) collected at 298 K on the pH of the sample. (B) Plot of pH dependence of the chemical shifts of peak 1 (□) and peak 2 (•). The data were fitted to theoretical curves, which yielded pK_{a1} = 7.12 ± 0.03 (blue line) and pK_{a2} = 7.04 ± 0.02 (red line). The uncertainties are those from curve fitting. We consider these pK_a values to be equal within experimental error.

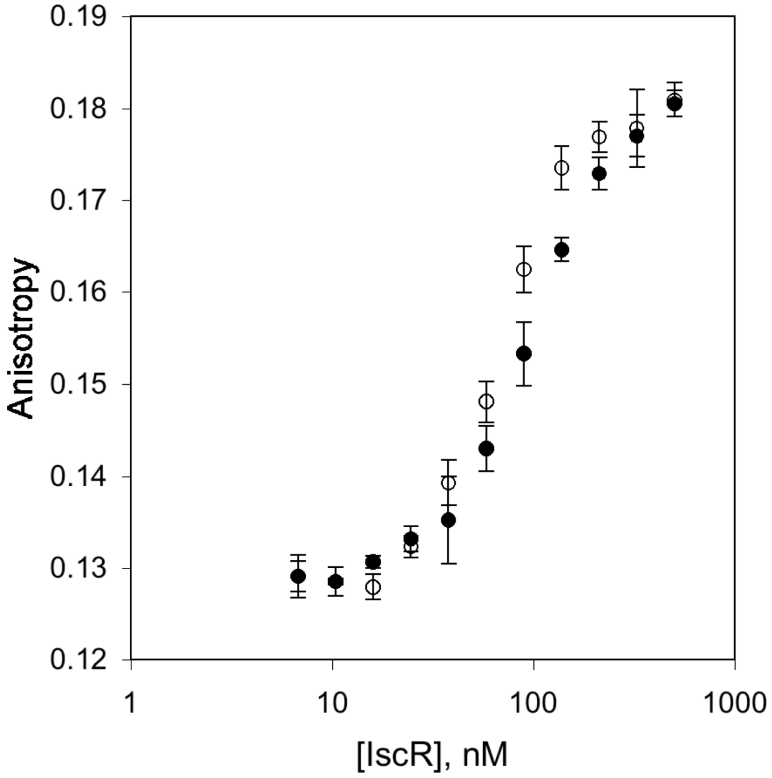

Figure 9.

In vitro DNA binding assays. As isolated IscR was exposed to oxygen and then tested for its ability to bind to double stranded DNA containing the *iscR* binding site in the absence (filled circles) or presence (open circles) of 10 μM dithionite.

Table 1

Mössbauer and EPR Parameters of Selected [2Fe-2S]$^{1+}$ Proteins

Parameters	**IscR**		***A. aeolicus* Fd1**[a]	
g values	1.88, 1.93, 1.99		1.88, 1.96, 2.05	
	Ferric site	Ferrous site	Ferric site	Ferrous site
δ (mm/s)	**0.33**	**0.70**	0.30	0.62
ΔE_q (mm/s)	**1.09**	**-3.4**	1.0	-3.0
η	**-0.5**	**-1.7**	0	-3
A_x (MHz)	**-53.5**	**8.9**	-56	11
A_y (MHz)	**-48.1**	**28.8**	-49	27
A_z (MHz)	**-44.6**	**30.2**	-42	33

[a]The [2Fe-2S] cluster of *A. aeolicus* Fd1 is ligated by four cysteines; Data from Meyer et al. (18)